tion with the use of an analog implementation of a rotation matrix (cos φ, sin φ, −sin φ, cos φ) acting on the scan voltages (W. Denk, unpublished data).
26. W. Denk, J. H. Strickler, W. W. Webb, *Science* **248**, 73 (1990).
27. W. Denk *et al.*, *J. Neurosci. Methods* **54**, 151 (1994).
28. W. Denk, D. W. Piston, W. W. Webb, in *Handbook of Biological Confocal Microscopy*, J. B. Pawley, Ed. (Plenum, New York, 1995), pp. 445–458.
29. Single-exponential behavior is predicted for equilibration between one well-mixed compartment (the spine head) and a large reservoir (the parent dendritic shaft) that are connected by a thin constriction. Because of its small size, the spine head is well mixed by diffusion for times greater than ~1 ms (*30*). Because of its large volume, the concentration in the shaft is almost unaffected by fluorophores diffusing into the head to replace those that have been bleached. Thus, when we bleached a spine, the fluorophore concentration in the adjacent shaft segment changed by ≤10%, and the change was largely attributable to bleaching from the tail of the point spread function, rather than to diffusional exchange—as was confirmed by repeating the experiment on a segment of shaft that lacked spines.
30. To determine the diffusion coefficient (D_f) for 3-kD FD in the internal solution, we released DMNB-caged FD (Molecular Probes) along a scan line and measured the time to peak (t_p) of the fluorescence intensity at a distance r. The equation $D_f = r^2/4t_p$ gave a D_f value of $1.0 \times 10^{-6} \pm 0.2 \times 10^{-6}$ cm^2/s, in agreement with previous estimates [M. Pusch and E. Neher, *Pfluegers Arch.* **411**, 204 (1988)]. In neuronal cytoplasm, the bulk diffusion coefficient is only 0.4×10^{-6} cm^2/s [S. Popov and M. Poo, *J. Neurosci.* **12**, 77 (1992)].
31. For two-photon fluorescence activation, cells were filled with 1 mM dimethoxy-nitro-benzyl (DMNB)–caged FD (3 kD). Exposure and measurement protocols were similar to those for photobleaching experiments (*25*). However, filling of cells was less reliable, and the low preactivation fluorescence level resulted in poor visibility and consequent difficulty in selecting spines. Small two-photon release cross sections (2×10^{-62} m^{4}s) (K. Svoboda, D. W. Tank, W. Denk, unpublished data) required longer exposure times (>12 ms). Although incidental in the photobleaching experiments, the longer wavelength of the monitor beam ensured that no additional release occurred during the decay period.
32. C. Koch and T. Poggio, *Proc. R. Soc. London B* **218**, 455 (1983).
33. The change in c_h is proportional to J and inversely proportional to V_h. Because the shaft is a large reservoir, c_s is constant and c_h obeys $V_h\, dc_h/dt = D_{FD}(c_h - c_s)/W_h$; the exponential time course for c_h follows.
34. To derive a crude estimate of spine neck length, we measured the smallest distance between the edges of the head and shaft, defined as the contour where the fluorescence intensity was one-half of the maximum. We then sorted our data into three categories according to head-shaft distance: <0.5 μm (Fig. 3D), 0.5 to 1.0 μm (Fig. 3C), and >1 μm (Fig. 3B).
35. Because spine head sizes are of the same order as or smaller than the optical resolution, we could not measure V_h geometrically from our images. Spine head volumes were measured as follows: The microscope point spread function, $f_{psf}(x, y, z)$, normalized so that $f_{psf}(0) = 1$, was measured with fluorescent latex spheres (diameter, 100 nm; Polysciences) injected into the slice at the appropriate depth. The spine head volume, V_h, was calculated as

$$V_h \iiint_{space} F(x,y,z)dxdydz \Big/ I_0 \iiint_{space} f_{psf}(x,y,z)dxdydz$$

where $F(x, y, z)$ is the measured fluorescence intensity and I_0 is a calibration intensity value measured inside a nearby dendritic shaft, large enough to contain most of the nonzero part of the point spread function.
36. K. M. Harris, F. E. Jensen, B. Tsao, *J. Neurosci.* **12**, 2685 (1992).
37. For large volumes, our distribution is similar to that obtained from SSEM measurements (maximum volumes: 0.56 μm^3, fluorescence; 0.55 μm^3, SSEM), but our smallest volumes are around 0.01 μm^3, compared with 0.004 μm^3 seen with SSEM. The brightness of the smallest spines was ~1% of that of the shaft, which renders them invisible with TPLSM and thus explains discrepancies in average volume (0.12 versus 0.051 μm^3) and average spine density (1.3 versus 2.5 per micrometer of dendrite) (*7*, *36*).
38. P. Fromherz and C. O. Müller, *Proc. Natl. Acad. Sci. U.S.A.* **91**, 4604 (1994).
39. G. Major, A. U. Larkman, P. Jonas, B. Sakman, J. J. B. Jack, *J. Neurosci.* **14**, 4613 (1994).
40. There are various uncertainties in our estimate of R_n: (i) Spines with relatively long necks were selected, which, together with the positive correlation between spine neck length and τ (Fig. 3, B to D), suggests that we overestimated the population average R_n. (ii) Estimates of ρ_i range from 200 to 400 ohm·cm (*37*, *38*). We used ρ_i = 250 ohm·cm; with ρ_i = 200 ohm·cm, R_n is decreased by a factor of 1.25, and with ρ_i = 400 ohm·cm R_n is increased by a factor of 1.6. (iii) Because 3-kD FD (hydrodynamic radius, ~2 nm) is a substantially larger particle than the ions responsible for cytoplasmic conductivity (primarily, K^+), a fine mesh of filaments in the spine neck could inhibit FD transport more than K^+ transport; if this is the case, we might have overestimated R_n. (iv) Cytoplasmic excluded volume (ϕ) due to proteins and organelles typically is between ~0.10 and 0.20 [F. Lanni, A. S. Waggoner, D. L. Taylor, *J. Cell Biol.* **100**, 1091 (1985)]. With a conservative upper bound of $\phi < 0.50$, given that some spines contain organelles (*7*), together with the other factors we find an absolute upper bound of R_n of ~150 megohms.
41. M. Baudry and J. L. Davis, Eds., *Long-Term Potentiation* (MIT Press, Cambridge, MA, 1994), vol. 2.
42. T. J. Sejnowski and N. Qian, in *Single Neuron Computation*, T. McKenna, J. Davis, S. F. Zornetzer, Eds. (Academic Press, Boston, 1992), pp. 117–139.
43. D. J. Linden, M. Smeyne, J. A. Connor, *Neuron* **11**, 1093 (1993).
44. J. M. Bekkers, G. B. Richerson, C. F. Stevens, *Proc. Natl. Acad. Sci. U.S.A.* **87**, 5359 (1990).
45. J. E. Lisman and K. M. Harris, *Trends Neurosci.* **16**, 141 (1993).
46. M. Raastad, J. F. Storm, P. Andersen, *Eur. J. Neurosci.* **4**, 113 (1992).
47. D. M. Kullmann and R. A. Nicoll, *Nature* **357**, 240 (1992).
48. B. Barbour, *Neuron* **11**, 759 (1993).
49. T. H. Brown, A. M. Zador, Z. F. Mainen, B. J. Claiborne, in *Single Neuron Computation*, T. McKenna, J. Davis, S. F. Zornetzer, Eds. (Academic Press, Boston, 1992), pp. 81–116.
50. We thank K. M. Harris, P. Mitra, and R. Yuste for helpful discussions.

13 November 1995; accepted 21 February 1996

Cell Growth Arrest and Induction of Cyclin-Dependent Kinase Inhibitor p21$^{WAF1/CIP1}$ Mediated by STAT1

Yue E. Chin,* Motoo Kitagawa,* Wu-Chou S. Su, Zhi-Hao You, Yoshiki Iwamoto, Xin-Yuan Fu†

Signal transducers and activators of transcription (STAT) proteins can be conditionally activated in response to epidermal growth factor (EGF) and interferon (IFN)–γ. STAT activation was correlated with cell growth inhibition in response to EGF and IFN-γ. Activated STAT proteins specifically recognized the conserved STAT-responsive elements in the promoter of the gene encoding the cyclin-dependent kinase (CDK) inhibitor p21$^{WAF1/CIP1}$ and regulated the induction of p21 messenger RNA. IFN-γ did not inhibit the growth of U3A cells, which are deficient in STAT1, but did inhibit the growth of U3A cells into which STAT1α was reintroduced. Thus, STAT1 protein is essential for cell growth suppression in response to IFN-γ. The STAT signaling pathway appears to negatively regulate the cell cycle by inducing CDK inhibitors in response to cytokines.

The cell cycle is controlled by a family of CDKs, which can be negatively regulated by families of CDK inhibitors (*1*) such as p21$^{WAF1/CIP1/CAP1}$ (*2*, *3*). An increase of the amount of p21 relative to the amount of cyclin-bound CDK may convert active CDK complexes into inactive ones (*1*, *4*). Some of the genes that control the cell cycle are assumed to be regulated by cytokine-induced signals. Nevertheless, the molecular basis for such signaling in responses to cytokines is not well defined. A signaling pathway exists in which tyrosine kinases phosphorylate and activate STAT proteins containing a conserved Src homology 2 (SH2) domain (*5*, *6*). The activated STAT proteins translocate from the cytoplasm to the nucleus (*6*, *7*), and many immediate-early responsive genes are thought to be regulated by activated STAT proteins and their partner proteins (*8*).

EGF often stimulates cell proliferation, whereas IFNs usually inhibit cell proliferation. However, the growth of A431 cells, which are derived from epidermoid carcinomas, is inhibited by EGF (*9*). EGF, like IFNs, can induce tyrosine phosphorylation and activation of STAT proteins (*10*–*12*), especially in A431 cells. We therefore de-

Department of Pathology, Yale University School of Medicine, New Haven, CT 06520–8023, USA.

*These authors contributed equally to this work.
†To whom correspondence should be addressed.

termined whether STAT activation by EGF correlated with suppression of cell growth. We used an electrophoretic mobility-shift assay (EMSA) to analyze many cell lines for STAT activation in response to EGF. STAT activation by EGF was very poor or absent in most cells except A431 cells (Fig. 1A) (*13*). In contrast to A431 cells, in which STAT1 and STAT3 proteins were activated (represented by SIFs, or sis-induced factors, in Fig. 1A) (*11*) and cell growth was inhibited in response to EGF treatment (Fig. 1B), no detectable STAT activation was observed after EGF treatment of HT29 and WiDr cells (Fig. 1A) (*13*), which are derived from human colon adenocarcinomas. HT29 and WiDr cells grew normally in the presence of EGF (Fig. 1, B to D). However, all these cells, including A431 cells, were responsive to IFN-γ and produced activated STAT1 (SIF-C) (Fig. 1A). The growth of all these cells was inhibited by IFN-γ treatment (Fig. 1, B to D). Results from a [^{3}H]thymidine incorporation assay were consistent with the growth curves (*14*). In many other cell lines, such as MCF7, HeLa S3, and PC12, STAT proteins were not activated by EGF treatment, although EGF treatment did induce phosphorylation of the receptor and activation of mitogen-activated protein (MAP) kinase (*14*); in these cells, growth was stimulated by EGF. Thus, STAT1 and STAT3 activation by EGF in A431 cells, and STAT1 activation by IFN-γ in most cells, correlates with the inhibition of cell growth.

To test whether activated STAT1 or STAT3, or both, participate in the control of cell growth by regulating certain genes encoding cell cycle mediators, we analyzed changes in expression of the genes encoding several CDKs, cyclins, and CDK inhibitors in response to EGF and IFN-γ. The p21 gene appears to be regulated directly by STAT proteins in response to EGF and IFN-γ. Three sequences in this promoter contain potential STAT-binding sites (*15*). These sites have been named p21-SIE1 (5′-CTTCCCGGAAG-3′), p21-SIE2 (5′-TTTCTGAGAAAT-3′), and p21-SIE3 (5′-CTTCTTGGAAAT-3′) (SIE, sis-inducible element) and are located at −640 nucleotides (nt), −2540 nt, and −4183 nt, respectively, from the TATA promoter site (*16*). All three potential SIE sites contain the palindromic sequence TTCNNNGAA usually present in STAT1-binding sites (*8*).

To verify whether these potential STAT-binding sites are actually recognized by STAT proteins in cells treated with EGF and IFN-γ, we performed EMSAs with each of the three p21-SIEs (Fig. 2). All three p21-SIEs formed stable complexes (originally termed SIF complexes) (*12, 15, 17*) with activated STAT proteins. We used p21-SIE1 as a probe to detect three SIF complexes (SIF-A, SIF-B, and SIF-C) in EGF-treated A431 cells (Fig. 2A). SIF-C and SIF-B were recognized and "supershifted" by antibody to STAT1 (anti-STAT1), whereas SIF-A and SIF-B were supershifted by anti-STAT3 (Fig. 2A). These observations indicate that SIF-A and SIF-C are probably composed of STAT1 and STAT3 homodimers, respectively, whereas SIF-B represents heterodimers of STAT1 and STAT3. No EGF-induced STAT activity was detected with the p21-SIE1 probe in HT29 or WiDr cells (Fig. 2A). These results were consistent with studies in which the classical STAT-binding probe M67-SIE was used (Fig. 1). However, A431, HT29, and WiDr cells were all responsive to IFN-γ treatment and generated the SIF-C complex with the p21-SIE1 probe (Fig. 2A), which was supershifted by anti-STAT1. Probes containing p21-SIE2 and p21-SIE3 were subjected to similar analyses. These two SIEs also formed a SIF complex preferentially with STAT1 (Fig. 2, B and C).

These results strongly indicate that these SIEs in the p21 promoter are binding sites for STAT proteins, thus raising the possibility that transcription of the p21 gene may be increased by STAT1 and STAT3 in response to EGF in A431 cells and in response to IFN-γ in many other cells. Transcription of p21 mRNA was rapidly increased (<30 min) in A431 cells treated with EGF, as measured by an RNA blotting analysis (Fig. 3A) (*18*). This increased

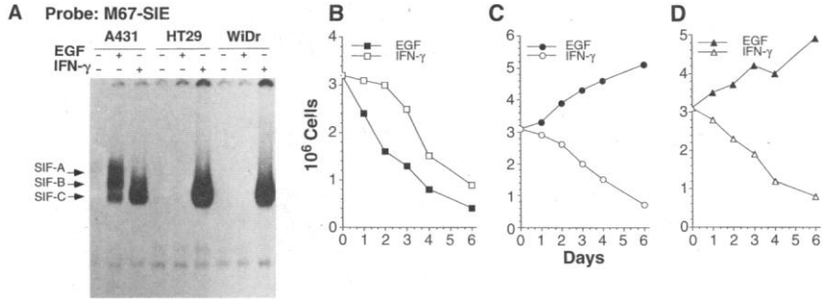

Fig. 1. STAT activation and cell growth inhibition in response to EGF or IFN-γ. (**A**) STAT complexes detected with the high-affinity STAT-binding site M67-SIE of the c-*fos* gene promoter (GTCGACATTTCCCGTAAATC) (*15*). Whole-cell extracts were prepared from either EGF-treated or IFN-γ–treated A431, HT29, or WiDr cells (*13*). Portions were assessed in EMSAs for the formation of SIF complexes (*13*). (**B** to **D**) Growth curves of A431 cells (B), HT29 cells (C), and WiDr cells (D). Cells (3×10^6) were treated with either EGF (100 ng/ml) or IFN-γ (160 ng/ml) for 1 to 6 days. Total viable cells were counted by the trypan blue dye–exclusion method. Data are averages of triplicate determinations.

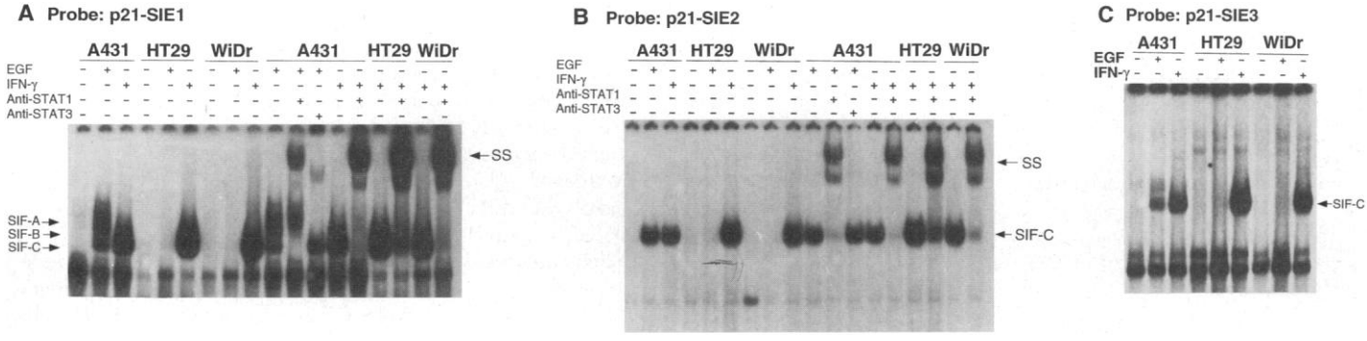

Fig. 2. Binding of STAT to the three SIE sites in the p21 promoter. Portions of whole-cell extracts prepared from EGF-treated or IFN-γ–treated A431, HT29, or WiDr cells were analyzed for SIF complex formation with p21-SIEs in an EMSA. The three p21-SIE probes used were p21-SIE1 (**A**), p21-SIE2 (**B**), and p21-SIE3 (**C**). In the supershift (SS) assays in (A) and (B), anti-STAT1 or anti-STAT3 was added to the reaction mixture before incubation with the probe. The probe sequences are as follows: p21-SIE1, 5′-GATCTCCTTCCCGGAAGCA-3′; p21-SIE2, 5′-GATCCTTTCTGAGAAATGG-3′; and p21-SIE3, 5′-GATCCCTCAGTCTTCTTGGAAATTC-3′ (*16*).

amount of p21 mRNA was maintained for at least 24 hours, a time course similar to that for activated STAT complexes induced by EGF in A431 cells (*14*). STAT proteins were not activated in WiDr cells in response to EGF, and the amount of p21 mRNA was not changed in these cells in response to EGF (Fig. 2B). IFN-γ activated STAT1 in A431, WiDr, and other cells (Fig. 2), and p21 mRNA was accordingly increased by IFN-γ (Fig. 3B) (*19*). These results suggest that STAT activation increases transcription of p21 mRNA in these cells. We made this element in a chloramphenicol acetyltransferase (CAT) reporter construct regulated by p21-SIE1 and analyzed its transcriptional regulation in response to IFN-γ in COS cells. The CAT activity of such cells treated with IFN-γ was eight times that in untreated cells (*20*). Therefore, p21-SIE1 is sufficient to allow transcriptional regulation induced by IFN-γ.

The mutant cell line U3A is defective in its response to IFNs and does not express STAT1 (*21*). If STAT1 is required for IFN-γ–induced cell growth arrest, then the growth of STAT1-deficient U3A cells should not be inhibited by IFN-γ. To test this hypothesis, we cotransfected U3A cells with the STAT1α expression vector pSG91 (*10*) and a vector containing a neomycin-resistance gene (*22*). The cell clones expressing STAT1 were selected and analyzed by STAT1 activation after treatment with IFN-γ (Fig. 4A). The control cells that had been transfected with an empty vector and the resistance gene (U3A-control) had no STAT activity in response to IFN-γ treatment. However, the active STAT1 complex (SIF-C) was induced in U3A cells that were transfected with STAT1 (Fig. 4A); these STAT1α-expressing U3A cells are denoted U3A-STAT1α. To compare rates of DNA synthesis, we measured the response of U3A-control and U3A-STAT1α cells to IFN-γ treatment (*23*). [^{3}H]Thymidine incorporation of U3A-control cells was not inhibited by IFN-γ, whereas that of U3A-STAT1α cells was inhibited (Fig. 4B). We also performed a colony-forming assay (*24*) with the U3A-control and U3A-STAT1α cells, which were originally derived from the human fibrosarcoma cell line HT1080 (*21*). Colony formation by U3A-STAT1α cells was inhibited by IFN-γ, whereas U3A-control cells were not affected (Fig. 4C). The p21 mRNA was expressed in larger amounts and was further induced in response to IFN-γ in U3A-STAT1α but not in U3A-control cells (*19*). Thus, STAT1 is apparently required in these cells for expression of p21 and suppression of cell growth in response to IFN-γ.

The CDK inhibitor p21 is probably encoded by one of the immediate-early genes, is activated within 30 min of cytokine treatment (Fig. 3A), and is induced directly by activated STAT1 and STAT3 proteins. This induction does not involve p53, because the amount of p53 was not altered in these cells after treatment with IFN-γ and EGF (*14*). Additionally, the p53 protein in A431 cells is mutated at codon 273 and is probably nonfunctional (*25*). The amount of p21 is increased and CDK2 activity is decreased during G_1 arrest in A431 cells (*26*). IFN-γ induces G_1 arrest in Daudi cells by inhibiting phosphorylation of retinoblastoma (Rb) protein (*27*), which is consistent with the effect of p21 in these cells (*1*, *28*).

Whether this p21 induction alone is sufficient for cell growth arrest, and how p21-SIEs are actually used in vivo (synergistically or individually), remains unknown. However, our results establish a link of the STAT signaling pathway to cell cycle control. There probably are more target genes in the cell cycle machinery, but we have tested the gene expression of almost all available CDKs, cyclins, and their inhibitors, and p21 appears to be the one that is strongly regulated by STAT.

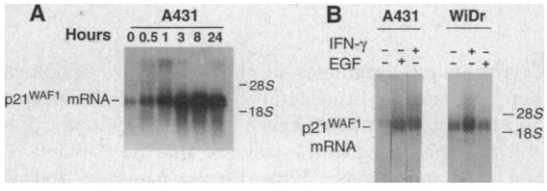

Fig. 3. Increased amount of p21 mRNA in cells treated with IFN-γ or EGF. (**A**) Increased amount of p21 mRNA in A431 cells treated with EGF. Cells were stimulated by EGF (100 ng/ml) for the indicated times and were collected for RNA isolation. RNA blotting analysis was done as described (*18*). The equality of the amount of RNA analyzed was verified by nonspecific staining with methylene blue. The x-ray film was exposed for 3 days. (**B**) Effects of IFN-γ or EGF on abundance of p21 mRNA in various cells. RNAs isolated from A431 or WiDr cells, incubated with or without IFN-γ (100 ng/ml) or EGF (100 ng/ml) for 24 hours, were assessed by blotting. The equality of the amount of RNA analyzed was verified by nonspecific staining with methylene blue. The x-ray film was exposed for 3 days.

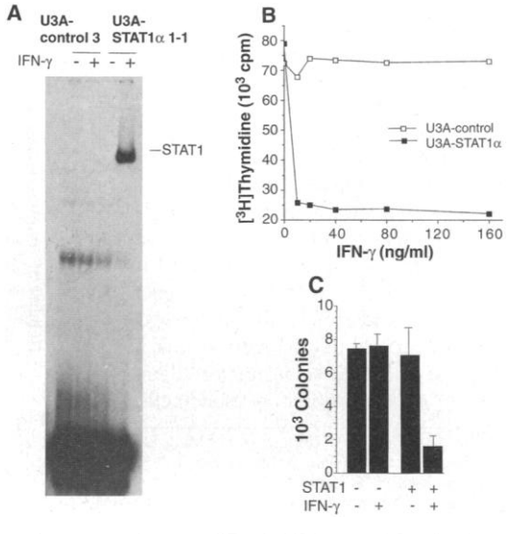

Fig. 4. Dependence of growth inhibition by IFN-γ on STAT1 in U3A cells. (**A**) Expression of STAT1 activity in U3A mutant cells. Extracts were prepared from U3A-control 3 cells or U3A-STAT1α 1-1 cells and incubated with or without IFN-γ (100 ng/ml) for 30 min. Protein (12 μg) was assessed for binding to the M67-SIE probe in each lane. (**B**) STAT1-dependent inhibition of U3A cell growth by IFN-γ. U3A-control 3 and U3A-STAT1α 1-1 cells (2×10^5 cells in each six-well microculture plate) were treated with various concentrations of IFN-γ for 24 hours and then assessed for their ability to incorporate [^{3}H]thymidine (*23*). The data are averages of triplicate determinations. (**C**) STAT1-dependent inhibition of colony formation of U3A cells by IFN-γ. The colony-formation assay was done as described (*24*) with or without IFN-γ. Colonies were counted on day 8. Each bar represents the average of the numbers of colonies in three plates; error bars are SDs. In U3A-control 3 cells, there was no difference in colony count between the treated and untreated groups, and in a different control clone, the results were essentially the same. However, a 77% reduction of colony formation was observed in U3A-STAT1α 1-1 cells and in two other STAT1-expressing clones treated with IFN-γ.

REFERENCES AND NOTES

1. T. Hunter and J. Pines, *Cell* **79**, 573 (1994); C. J. Sherr and J. M. Roberts, *Genes Dev.* **9**, 1149 (1995).
2. W. S. El-Deiry *et al.*, *Cell* **75**, 817 (1993); Y. Gu, C. W. Turck, D. O. Morgan, *Nature* **366**, 707 (1993); J. W. Harper, G. R. Adami, N. Wei, J. Keyomarsi, S. J. Elledge, *Cell* **75**, 805 (1993).
3. Y. Xiong *et al.*, *Nature* **366**, 701 (1993).
4. H. Zhang, G. J. Hannon, D. Beach, *Genes Dev.* **8**, 1750 (1994); J. W. Harper *et al.*, *Mol. Biol. Cell* **6**, 387 (1995).
5. X.-Y. Fu, *Cell* **70**, 323 (1992); C. Schindler, K. Shuai, V. R. Prezioso, J. E. Darnell Jr., *Science* **257**, 809 (1992); L. Velazquez, M. Fellous, G. R. Stark, S. Pellegrini, *Cell* **70**, 313 (1992); M. J. Gutch, C. Daly, N. C. Reich, *Proc. Natl. Acad. Sci. U.S.A.* **89**, 11411 (1992); M. Müller *et al.*, *Nature* **366**, 129 (1993); A. C. Larner *et al.*, *Science* **261**, 1730 (1993).
6. J. E. Darnell Jr., I. M. Kerr, G. R. Stark, *Science* **264**, 1415 (1994); X.-Y. Fu, *J. Leukocyte Biol.* **57**, 529 (1995); J. N. Ihle, *Nature* **377**, 591 (1995); M. Karin and T. Hunter, *Curr. Biol.* **5**, 747 (1995).
7. D. E. Levy, D. S. Kessler, R. Pine, J. E. Darnell Jr., *Genes Dev.* **3**, 1362 (1989); X.-Y. Fu, D. S. Kessler, S. A. Veals, D. E. Levy, J. E. Darnell Jr., *Proc. Natl. Acad. Sci. U.S.A.* **87**, 8555 (1990); D. S. Kessler, S. A. Veals, X.-Y. Fu, D. E. Levy, *Genes Dev.* **4**, 1753 (1990); X.-Y. Fu, C. Schindler, T. Improta, R. Aebersold, J. E. Darnell Jr., *Proc. Natl. Acad. Sci. U.S.A.* **89**, 7840 (1992).
8. X.-Y. Fu, in *Inducible Gene Expression*, P. Bauerle, Ed. (Birkhauser, Boston, 1995), vol. 2, pp. 99–130.
9. G. N. Gill and C. S. Lazar, *Nature* **293**, 305 (1981); R.

Bravo, J. Burckhardt, T. Curran, R. Müller, *EMBO J.* **4**, 1193 (1985).
10. X.-Y. Fu and J.-J. Zhang, *Cell* **74**, 1135 (1993).
11. S. Ruff-Jamison, K. Chen, S. Cohen, *Science* **261**, 1733 (1993); S. Ruff-Jamison *et al.*, *J. Biol. Chem.* **269**, 21933 (1994); H. B. Sadowski and M. Z. Gilman, *Nature* **362**, 79 (1993).
12. Z. Zhong, Z. Wen, J. E. Darnell Jr., *Science* **264**, 95 (1994).
13. A431 cells from the American Type Culture Collection (ATCC CRL-1555) were grown in Dulbecco's modified Eagle's medium (DMEM) with calf serum (10%). HT29 cells (ATCC HTB-38) were grown in McCoy's 5A medium with fetal bovine serum (FBS) (10%). WiDr cells (ATCC CLL-218) were grown in minimal essential medium with FBS (10%). Human recombinant EGF was obtained from Gibco BRL, IFN-γ from Genentech, and antibodies to STAT1 and STAT3 from Santa Cruz Biotechnology. Whole-cell extracts were prepared as described (*10*) by lysis of cells in 20 mM Hepes (pH 7.9) buffer containing 0.2% NP-40, 10% glycerol, 400 mM NaCl, 0.1 mM EDTA, 1 mM dithiothreitol, 1 mM sodium vanadate, 0.5 mM phenylmethylsulfonyl fluoride, and aprotinin, leupeptin, and pepstatin (1 μg/ml of each). For EMSAs, double-stranded oligodeoxynucleotide probes were end-labeled with [γ-^{32}P]ATP and portions equivalent to 20,000 cpm were used per reaction. Binding reactions were performed in a total volume of 15 μl in 10 mM Hepes (pH 7.9), 0.1 mM EDTA, 5% glycerol, poly(deoxyinosine-deoxycytidine) (50 μg/ml, Pharmacia), and 0.01% NP-40. Extracts were incubated for 10 min on ice, antibody (1 μl) was added followed by an additional 30-min incubation on ice, and then the end-labeled DNA probe was added and incubated for 20 min at room temperature. Complexes were separated on nondenaturing acrylamide gels (6%) in 0.5× tris-borate EDTA and detected by autoradiography.
14. Y. E. Chin and X.-Y. Fu, unpublished data.
15. B. J. Wagner, T. E. Hayes, C. J. Hoban, B. H. Cochran, *EMBO J.* **9**, 4477 (1990).
16. W. S. El-Deiry *et al.*, *Cancer Res.* **54**, 1169 (1994).
17. H. B. Sadowski, K. Shuai, J. E. Darnell Jr., M. Z. Gilman, *Science* **261**, 1739 (1993).
18. Total cellular RNA was prepared by the guanidinium thiocyanate–CsCl procedure. RNA (5 mg) was separated on a 1.0% agarose-formaldehyde gel and transferred onto a nylon membrane (Zeta-Probe, Bio-Rad). The filter was stained with methylene blue [D. L. Herrin and G. W. Schmidt, *Biotechniques* **6**, 196 (1988)] and then hybridized at 65°C in 0.25 M Na_2PO_4 (pH 7.2), 7% SDS, and 1 mM EDTA. The wash was performed at 65°C in 0.04 M Na_2PO_4 (pH 7.2) and 1% SDS. The probe was prepared by labeling a Stu I–Xho I fragment (1.9 kb) of human p21 complementary DNA (*3*) with the use of a random-primed DNA labeling kit (Boehringer Mannheim).
19. M. Kitagawa, W.-C. S. Su, X.-Y. Fu, unpublished data.
20. Z.-H. You and X.-Y. Fu, unpublished data.
21. R. McKendry *et al.*, *Proc. Natl. Acad. Sci. U.S.A.* **88**, 11455 (1991); M. Müller *et al.*, *EMBO J.* **12**, 4221 (1993).
22. U3A cells (*21*) were transfected with 0.3 μg of pSTneoB linearized with Xho I [K. Katoh, Y. Takahashi, S. Hayashi, H. Kondoh, *Cell Struct. Funct.* **12**, 575 (1987)] and 15 μg of either pSG5 (Stratagene) or pSG91 (*10*) linearized with Sal I by the calcium phosphate method [F. M. Ausubel *et al.*, *Current Protocols in Molecular Biology* (Wiley-Interscience, New York, 1987)]. G418-resistant cells were selected and maintained in medium containing G418 (700 μg/ml).
23. The cells (2 × 10^5 cells in a six-well microculture plate) treated with EGF or IFN-γ were incubated with [^{3}H]thymidine (5 μCi/ml) for 6 hours. Cells were then washed twice with phosphate-buffered saline, harvested onto the glass filters, and added to vials containing scintillation fluid for liquid-scintillation measurement of ^{3}H incorporation.
24. A two-layer soft-agar system was prepared by plating 0.5% agar in DMEM containing calf serum (20%) in 60-mm dishes [A. W. Hamburger and S. E. Salmon, *Science* **197**, 461 (1977)]. Cells were passed through a 25-gauge needle and then suspended in a 0.35% agar solution in DMEM enriched with calf serum (20%). The final concentration of cells in 0.35% agar solution was 2.5 × 10^4 cells/ml in 2 ml (5 × 10^4 cells). Plates were examined immediately after plating, to ensure that a single-cell suspension in agar had been achieved, and were then incubated. All specimens were plated in triplicate. DMEM (0.2 ml) containing calf serum (10%) was added to each well. IFN-γ was added to the final plating mixture just before plating (final concentration, 100 ng/ml), but not to control plates. IFN-γ was then added daily after plating to maintain the effect. Colonies were counted (a colony was defined as a new round aggregate of 50 or more cells) on day 8 with a phase-contrast inverted microscope.
25. T. Kwok, T. Mok, C. H. Menton-Brennan, *Cancer Res.* **54**, 2834 (1994).
26. Z. Fan *et al.*, *J. Cell Biol.* **131**, 235 (1995).
27. D. Resnitzky, N. Tiefenbrun, H. Berissi, A. Kimchi, *Proc. Natl. Acad. Sci. U.S.A.* **89**, 402 (1992).
28. We thank G. R. Stark and I. M. Kerr for the U3A cell line; Y. Xiong for p21 cDNA; Genentech for IFN-γ; W.-F. Tao for some of the cells; D. Stern, D. Bregman, and H. Zhang for critical reading of the manuscript and helpful discussions; N. Bennett for assistance in preparing the manuscript; and colleagues in our department for support. Supported by grants from the American Cancer Society (NP883), NIH (RO1 AI 34522), and the Council for Tobacco Research (4238) to X.-Y.F. Y.E.C. is supported by a NIH training grant.

26 January 1996; accepted 6 March 1996

In Vitro Development of Primitive and Definitive Erythrocytes from Different Precursors

Toru Nakano,* Hiroaki Kodama, Tasuku Honjo

During mouse embryogenesis the production of "primitive" erythrocytes (EryP) precedes the production of "definitive" erythrocytes (EryD) in parallel with the transition of the hematopoietic site from the yolk sac to the fetal liver. On a macrophage colony-stimulating factor–deficient stromal cell line OP9, mouse embryonic stem cells were shown to give rise to EryP and EryD sequentially with a time course similar to that seen in murine ontogeny. Studies of the different growth factor requirements and limiting dilution analysis of precursor frequencies indicate that most EryP and EryD probably developed from different precursors by way of distinct differentiation pathways.

Erythropoiesis originates in the yolk sac, then migrates to the fetal liver during mouse embryogenesis. EryP and EryD, which are produced in the yolk sac and the fetal liver, respectively, have distinct morphological and biochemical characteristics (*1*, *2*). Whether these two cell types develop from a single common hematopoietic precursor or not has been the subject of controversy (*3*, *4*). To address this question, we used the in vitro differentiation induction system of embryonic stem (ES) cells to hematopoietic cells (*5*).

Two waves of erythroid cell production were observed when D3 ES cells were cocultured with OP9 stromal cells (Fig. 1A) (*5*–*8*). The first wave of erythropoiesis appeared at day 6 of the induction, and all of the day 7 erythroid lineage cells were large-nucleated cells morphologically identical to EryP (Fig. 2A). The number of erythroid lineage cells suddenly decreased at days 8 and 9 to less than one-fifth of that at day 7. Subsequently, the second wave of erythroid lineage cells appeared around day 10 with a peak at day 14; these cells were small-nucleated erythroblasts or enucleated mature blood cells morphologically identical to EryD (Fig. 2B). In agreement with the report that EryP contain not only embryonic ζ- and ε-globin but also adult α-globin, whereas EryD contain only adult α- and β-globins (*9*), day 7 erythroid lineage cells were positive for staining with antibodies against embryonic as well as against adult hemoglobins, whereas day 14 erythroid cells were positive for staining with antibodies against adult hemoglobin only (Fig. 2, C to F) (*10*–*12*). Expression of ζ-, α-, and ε-globin mRNA in day 7 erythrocytes

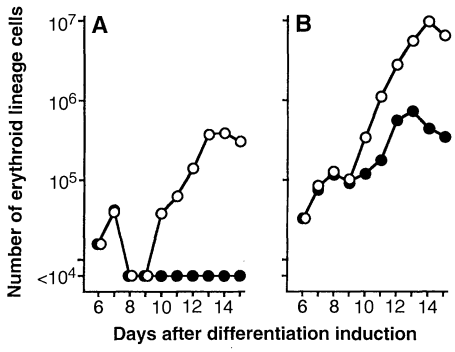

Fig. 1. Development of erythroid lineage cells during differentiation induction of D3 ES cells on OP9 stromal cells, and effects of anti–c-Kit (Ack2) and erythropoietin (EPO) on the development (*24*). Differentiation induction of ES cells was done without (**A**) or with (**B**) the addition of exogenous human recombinant EPO (10 U/ml) (*8*). Data are shown in the absence (○) or presence (●) of Ack2 (10 μg/ml).

T. Nakano and T. Honjo, Department of Medical Chemistry, Faculty of Medicine, Kyoto University, Yoshida, Sakyo-ku, Kyoto 606, Japan.
H. Kodama, Department of Anatomy, Ohu University School of Dentistry, Tomitamachi, Koriyama, Fukushima 963, Japan.

*Present address: Department of Molecular Cell Biology, Research Institute for Microbial Diseases, Osaka University, Yamada-Oka, Suita, Osaka 565, Japan.